Refined Analysis of the Thermal Dissociation of Formaldehyde†

J. Troe

Institut für Physikalische Chemie, Universität Göttingen, Tammannstrasse 6, D-37077 Göttingen, Germany

Received: October 6, 2006; In Final Form: November 10, 2006

New experimental results for the thermal dissociation of formaldehyde to radical and molecular products (*Proc. Combust. Inst.* **2007**, *31*, in press) form the basis of the present analysis of the respective low-pressure rate coefficients $k_{Rad,0}$ and $k_{Mol,0}$ of the reaction. The article supersedes an earlier analysis (*J. Phys. Chem. A* **2005**, *109*, 8320) which used less accurate and more preliminary input information. In addition, refined rotational factors F_{rot} are determined and specific energy and angular momentum dependent branching ratios from a more detailed analysis of photolysis quantum yields (*J. Phys. Chem. A* **2007**, *111*, 3868) are employed as well. It is emphasized again that pyrolysis and photolysis are intimately related and should be analyzed in an internally consistent manner. The combination of the new with earlier experimental results for pyrolysis rates allows one to fit the height of the energy barrier for the molecular elimination channel with improved precision. A value of $E_{0,1} = 81.7(\pm 0.5)$ kcal mol^{-1} is obtained. In addition, employing anharmonicity factors F_{anh} from the earlier work, a total average energy transferred per collision of $-\langle\Delta E\rangle/hc = 100(\pm 20)$ cm^{-1} is fitted from the experiments in the bath gas Ar. This value is consistent with the value $-\langle\Delta E\rangle/hc = 80(\pm 40)$ cm^{-1} for the bath gas N_2 such as fitted from photolysis quenching experiments (using the same molecular parameters as for the pyrolysis). Rate coefficients for the temperature range 1200−3500 K are represented in the form $k_{Mol,0}/[Ar] = 7.3 \times 10^{14}\ T^{-6.1} \exp(-47300\ K/T)$ cm^3 molecule^{-1} s^{-1} and $k_{Rad,0}/[Ar] = 2.1 \times 10^{12}\ T^{-5.5} \exp(-47300\ K/T)$ cm^3 molecule^{-1} s^{-1} (accuracy ±25%) and recommended for use in combustion chemistry.

I. Introduction

The dissociation of formaldehyde presents an attractive example of a multichannel unimolecular reaction. There is the molecular elimination process

$$H_2CO \rightarrow H_2 + CO \quad (1)$$

which competes with the radical-forming dissociation

$$H_2CO \rightarrow H + HCO \quad (2)$$

In addition, it has been shown[1−5] that molecular products are also formed via a "third channel" of the intramolecular hydrogen-abstraction type

$$H_2CO \rightarrow H\cdots HCO \rightarrow H_2 + CO \quad (3)$$

the so-called "roaming atom pathway". Channel 3 opens up at the threshold energy of channel 2 and has dynamical properties which distinctly differ from those of channel 1. However, above this threshold energy channels 1−3 also appear to be coupled, and it remains an open question to what extent they really can be separated.

The dissociation of formaldehyde can be studied by thermal and by photochemical excitation. Because electronic excitation in the latter case is followed by fast internal conversion to the electronic ground state, pyrolysis and photolysis of formaldehyde are intimately linked and, therefore, should be analyzed in a consistent manner. On the basis of this assumption, the pyrolysis of formaldehyde was analyzed earlier by the present author,[6] employing information on the relative importance of channels 1−3, which was derived from a preliminary analysis of photolysis quantum yields[7−11] and from modeling of the branching by classical trajectory calculations.[3,4] At the same time experimental low-pressure rate constants for the formation of molecular and radical products were used.[12−17] An important result from this analysis was the conclusion that the threshold energy of channel 1 must be markedly higher than assumed initially.[18] This observation confirmed results from quantum-chemical calculations[19] which also questioned the conclusions about the threshold energy drawn in ref 18.

The reason why the present author after the publication of ref 6 comes back so soon to the analysis of thermal dissociation rates of formaldehyde is multiple. First, his new and more detailed analysis of photolysis quantum yields[20] led to more specific information about the energy and angular momentum dependence of the branching between channels 1−3. Second, more reliable experimental information on the molecular channel 1 in the pyrolysis has become available recently.[21] Third, the rotational channel switching properties of the present reaction system were found to require a more accurate treatment of the rotational factor F_{rot} in the low-pressure rate constant than given in the previous analysis[6] where the standard single-channel approximation from ref 22 was employed. Fourth, the present refined analysis of the rate constant leads to a more reliable value of the average energy $\langle\Delta E\rangle$ transferred per collision which now more safely can be compared with a value derived from photolysis quenching experiments; see ref 20. As a new theoretical modeling of the branching by trajectory calculations is also underway,[5,23] it appears desirable to provide a refined and internally consistent analysis of pyrolysis and photolysis experiments such as given in the following article for the pyrolysis and in ref 20 for the photolysis. This study allows one to extrapolate experimental rate coefficients for pyrolysis and photolysis quantum yields into ranges of conditions which

† Part of the special issue "James A. Miller Festschrift".

10.1021/jp0665675 CCC: $37.00
Published on Web 02/01/2007

so far have not been studied experimentally. A small difference between the energy and angular momentum dependent branching ratios derived from pyrolysis and photolysis experiments appears to be noticeable which may indicate some differences in the specific excitation pathways and which may also correspond[20] to fine structures in the quantum yields such as detected in ref 24.

II. Specific Branching Ratios

The dissociaton of formaldehyde to a large extent is governed by rotational channel switching.[6] At small values of the quantum numbers J of the total angular momentum, channel 1 has the lower threshold energy, being denoted by $E_{0,1}(J)$. At large values of J, the threshold energy $E_{0,2}(J)$ of channels 2 and 3 becomes smaller than $E_{0,1}(J)$. The values of $E_{0,1}(J)$ and $E_{0,1}(J)$ sensitively influence the branching ratio between molecular and radical products and, therefore, have to be characterized as quantitatively as possible.

Putting the zeropoint of the energy scale at the rovibrational ground state of H_2CO, $E_{0,1}(J)$ can be represented by

$$E_{0,1}(J) \approx E_{0,1}(J=0) + B^{\neq}\mathrm{hc}J(J+1) \qquad (4)$$

with an effective rotational constant $B^{\neq}$ of the energy barrier of channel 1; see below. $E_{0,1}(J=0)$ in ref 6 was fitted from the experimental branching ratios of the pyrolysis. As these ratios also depend on less well-known details of the J dependence of the specific branching ratios, a different policy is followed in the present work where the now particularly well characterized experimental temperature dependence of radical formation rates provides a more accurate basis for the fit. A value of $E_{0,1}(J=0)/\mathrm{hc} = 28\,570(\pm 200)$ cm^{-1} (corresponding to $E_{0,1}(J=0) = 81.7(\pm 0.5)$ kcal mol^{-1}) is derived, see below, which is also consistent with the value of $E_{0,1}(J=0)/\mathrm{hc} = 28\,645(\pm 100)$ cm^{-1} (corresponding to $E_{0,1}(J=0) = 81.9(\pm 0.3)$ kcal mol^{-1}) recommended in ref 19. The threshold energy $E_{0,2}(J)$ for channels 2 and 3 has a much weaker J dependence which, over the range of relevance here, can be approximated by an expression of the form

$$E_{0,2}(J) \approx E_{0,2}(J=0) + C_\nu \mathrm{hc}[J(J+1)]^\nu \qquad (5)$$

The parameters $B^{\neq}$, C_ν, and ν are determined from the ab initio calculations of the potential, see refs 19 and 25−29, and are taken as $B^{\neq} = 1.11$ cm^{-1}, $C_\nu = 0.43$ cm^{-1}, and $\nu = 1.0$. The value of $E_{0,2}(J=0)$ is known with spectroscopic precision to be[30,31] $E_{0,2}(J=0)/\mathrm{hc} = 30\,328.5(\pm 0.5)$ cm^{-1} (corresponding to $E_{0,2}(J=0) = 86.71(\pm 0.0015)$ kcal mol^{-1}). The switching value J_{sw} of J, where channel 1 changes from the energetically more to the less favorable channel (tunneling neglected), is close to $J_{sw} \approx 48$.

Radical products can only be formed when $E \geq E_{0,2}(J)$. At the same time, there is formation of molecular products through channels 1 and 3. Unlike ref 6, we do not separate channels 1 and 3 in this range but combine them into one branching ratio which directly also enters into the experimental photolysis quantum yields.[6,20] We employ energy E-specific and angular momentum J-specific branching ratios $V_{Rad}(E,J)$ and $V_{Mol}(E,J)$ for the formation of radical and molecular products, respectively (with $V_{Mol}(E,J) = 1 - V_{Rad}(E,J)$). Thermal averages over $V_{Rad}(E,J)$ determine the photolysis quantum yields for radical formation in the spectral range 310−340 nm. $V_{Rad}(E)$ and $V_{Mol}(E)$ have been calculated by classical trajectories for $J = 0$ in ref 3 while a separation into $V_1(E)$, $V_2(E)$, and $V_3(E)$ was provided in ref 5. A further refinement accounting for a J dependence of $V_{Rad}(E,J)$ and of $V_{Mol}(E,J)$ was suggested in refs 6 and 20 on the basis of experimental photolysis quantum yields. Trajectory calculations of the J dependence of the branching ratio are also underway.[23] An expression of the form of

$$V_{Rad}(E,J) \approx C_1\{1 - \exp[-C_2 J - \{[E - E_{0,2}(J)]/C_3\}]\} \qquad (6)$$

was proposed in ref 20 with the parameters $C_1 \approx 0.75$, $C_2 \approx 0.05$, and $C_3/\mathrm{hc} \approx 750$ cm^{-1}. While C_1 and C_3 were given by the trajectory calculations from ref 3, being consistent with the measured quantum yields, the value of C_2 was only fitted from the experimental quantum yields. If formaldehyde is represented as a symmetric top, such as was done throughout this article, no dependence of $V_{Rad}(E,J)$ on the quantum number K was taken into consideration.

III. Modeled Total Low-Pressure Rate Coefficients

Under typical experimental conditions, the pyrolysis shows second order behavior; see, e.g., ref 17. Tunneling contributions, which broaden the falloff curves and make the true low-pressure limit unattainable, have been shown not to play a significant role under these conditions.[32] Deviations from second order behavior so far have not been observed experimentally up to the highest applied pressures (such as used in ref 33). Therefore, here we only consider the "normal" low-pressure dissociation rate constant as expressed in standard form[22] by

$$k_0/[\mathrm{M}] \approx \beta_c Z_{LJ}[\rho_{vib,h}(E_0)\mathrm{k}T/Q_{vib}]\exp(-E_0/\mathrm{k}T)F_E F_{anh} F_{rot} \qquad (7)$$

with E_0 defined by $E_{0,1}(J=0)$, see the theory of two-channel thermal unimolecular reactions from ref 34. k_0 denotes the total dissociation rate constant given by the sum of contributions from the channels 1−3; i.e. $k_0 = k_{1,0} + k_{2,0} + k_{3,0}$.

The J dependence of $E_{0,1}(J)$ and $E_{0,2}(J)$ in ref 6 was accounted for by using the approximate rotational factor F_{rot} from ref 22. In the present work the J dependence is treated more accurately by the detailed calculation of F_{rot} in the form

$$F_{rot} \approx \sum_{J=0}^{\infty}(2J+1)\sum_{K=-J}^{+J}{}^*\{\rho_{vib,h}[E_{0,min}(J) - E_{rot}(J,K)]/\rho_{vib,h}(E_0)\} \times \exp\{-[E_{0,min}(J) - E_0]/\mathrm{k}T\}/\sum_{J=0}^{\infty}(2J+1)\sum_{K=-J}^{+J}\exp\{-E_{rot}(J,K)/\mathrm{k}T\} \qquad (8)$$

where

$$E_{0,min}(J) = \min[E_{0,1}(J), E_{0,2}(J)] \qquad (9)$$

and $E_0 = E_{0,1}(J{=}0)$ (Σ^* means that the summation extends over the range $E_{rot}(J,K) \leq E_{0,min}(J)$ only). The differences between the present and the earlier calculations of F_{rot} will be illustrated below.

The analysis of the experimental total low-pressure rate constants for formation of molecular and radical products on the basis of eq 7 can lead to two quantities: when the temperature dependence of k_0, or one of the two quantities $k_{2,0} = k_{Rad,0}$ and $k_{1,0} + k_{3,0} = k_{Mol,0}$, is known from accurate measurements over a wide temperature range, one can fit $E_0 = E_{0,1}(J=0)$. Having fixed E_0, the absolute value of k_0 then leads to an experimental value of the collision efficiency β_c and, through the analytical solution of the master equation from ref

35, from β_c to the average (total) energy transferred per collision $\langle\Delta E\rangle$; see below. The molecular parameters used in eq 7, in addition to those specified later on, are given in the Appendix of ref 6.

IV. Modeled Low-Pressure Thermal Branching Ratios

In order to obtain individual low-pressure rate coefficients for the formation of radical and molecular products, a more specific treatment is required. It has to account for three essential phenomena: (i) rotational channel switching, (ii) branching between radical and molecular products at $E \geq E_{0,2}(J)$, and (iii) nonequilibrium populations of molecular states such as described by solution of the master equation for multichannel thermal unimolecular reactions.[34] Points i and ii were elaborated on in section II. Point iii is taken into account as described as follows.

As long as details of rovibrational collisional energy transfer are not characterizable in detail, the two-dimensional master equation of the collisional activation-dissociation sequence should be treated in a decoupled way, i.e., by solving one-dimensional master equations for each individual J and summing up the resulting partial contributions to the rate coefficient assuming an equilibrium distribution of rotational states. As in ref 34, we follow this concept using the analytical solution of the master equation for an exponential collision model such as elaborated in ref 35. In this treatment the nonequilibrium population factor $h(E,J)$, given by the ratio of the nonequilibrium population $g(E,J)$ and the equilibrium population $f(E,J)$, at energies E above the threshold energies $E_{0,\min}(J)$ from eq 9, in the low-pressure range is given by

$$h(E,J) \approx \{Z_{LJ}[M]/[k_1(E,J) + k_2(E,J) + k_3(E,J)]\}\{\alpha/(\alpha + F_E kT)\}\exp\{-[E - E_{0,\min}(J)]/\alpha\} \quad (10)$$

α here denotes the average energy transferred per down collision. The low-pressure rate coefficient $k_{Rad,0}$ for the formation of radical products from this is calculated through

$$k_{Rad,0} = \sum_{J=0}^{\infty} (2J+1) \int_{E_{0,\min}(J)}^{\infty} k_2(E,J)h(E,J)f(E,J)\,dE \quad (11)$$

which, with the branching ratio

$$V_{Rad}(E,J) = k_2(E,J)/[k_1(E,J) + k_2(E,J) + k_3(E,J)] \quad (12)$$

from eq 6, leads

$$k_{Rad,0} \approx Z_{LJ}[M]\{\alpha/(\alpha + F_E kT)\}\sum_{J=0}^{\infty} (2J+1) \int_{E_{0,\min}(J)}^{\infty} V_{Rad}(E,J)\exp\{-[E - E_{0,\min}(J)]/\alpha\}f(E,J)\,dE \quad (13)$$

Within this approach, the equilibrium population $f(E,J)$ is represented by

$$f(E,J) \approx (Q_{vib}Q_{rot})^{-1}\rho_{vib,h}(E_0)\exp(-E_0/kT)F_E F_{anh} \sum_{K=-J}^{+J} {}^*\{\rho_{vib,h}[E_{0,\min}(J) - E_{rot}(J,K)]/\rho_{vib,h}(E_0)\} \times \exp\{-[E - E_{0,\min}(J)]/kT\} \quad (14)$$

As before, E_0 is defined by $E_0 = E_{0,1}(J = 0)$. The energy dependence of $\rho_{vib,h}(E,J)$ is approximately accounted for by the factor F_E and F_{anh} corresponds to anharmonicity contributions at $E \approx E_0$; see Appendix of ref 6. The collisional energy transfer parameter α, within the exponential collision model, is related to the total average energy transferred per collision $\langle\Delta E\rangle$ by[35]

$$\langle\Delta E\rangle \approx \alpha^2/(\alpha + F_E kT) \quad (15)$$

Replacing $V_{Rad}(E,J)$ by unity, eqs 13−15 lead to eq 7 with[35]

$$\beta_c = [\alpha/(\alpha + F_E kT)]^2 \quad (16)$$

i.e., one recovers the conventional expression for the low-pressure rate coefficient such as described in detail in ref 22.

Employing the Whitten−Rabinovitch expression for $\rho_{vib,h}(E)$ and using $F_{anh} \approx 1.89$, such as estimated in ref 6 (Appendix), the numerical evaluation of eqs 13−16 is straightforward. On the basis of the experimental information for the temperature dependence of $k_{Rad,0}(T)$ which is available over a large temperature range, and for the ratio $k_{Rad,0}/k_0$ and the absolute value of k_0 which is available over a small temperature range (see below), one may then fit the three parameters $E_{0,1}(J = 0)$, $\langle\Delta E\rangle$, and C_2 such as was done in the following sections.

V. Evaluation of Experimental Results

We base the present analysis of experimental results on the new measurements from ref 21 which, over the temperature range 2258−2687 K and with an uncertainty of about ±25%, gave

$$k_{Rad,0} = [\mathrm{Ar}]\ 9.71 \times 10^{-10}\exp(-32100\ \mathrm{K}/T)\ \mathrm{cm^3\ molecule^{-1}\ s^{-1}} \quad (17)$$

and

$$k_{Mol,0} = [\mathrm{Ar}]\ 7.70 \times 10^{-10}\exp(-28700\ \mathrm{K}/T)\ \mathrm{cm^3\ molecule^{-1}\ s^{-1}} \quad (18)$$

Figure 1 illustrates the results from ref 21. While the value of $k_{Rad,0}(2500\ \mathrm{K}) = [\mathrm{Ar}]\ 2.6 \times 10^{-15}\ \mathrm{cm^3\ molecule^{-1}\ s^{-1}}$ agrees well with the average of the earlier results from refs 12, 13, 15, and 17, the new value of $k_{Mol,0}(2500\ \mathrm{K}) = [\mathrm{Ar}]\ 8.5 \times 10^{-15}\ \mathrm{cm^3\ molecule^{-1}\ s^{-1}}$ essentially coincides with that of $k_{Mol,0} \approx [\mathrm{Ar}]\ 6.8 \times 10^{-15}\ \mathrm{cm^3\ molecule^{-1}\ s^{-1}}$ from the unpublished data of ref 12, but is markedly lower than $k_{Mol,0}(2500\ \mathrm{K}) = [\mathrm{Kr}]\ 1.8 \times 10^{-14}\ \mathrm{cm^3\ molecule^{-1}\ s^{-1}}$ from ref 16, which was preferred in our earlier analysis.[6]

Earlier experiments[17] from the same laboratory as ref 21 enlarge the temperature range of experimental data for $k_{Rad,0}$. Over the range 1675−2080 K values of

$$k_{Rad,0} = [\mathrm{Ar}]\ 8.3 \times 10^{-9}\exp(-37044\ \mathrm{K}/T)\ \mathrm{cm^3\ molecule^{-1}\ s^{-1}} \quad (19)$$

were obtained. Figure 2 illustrates the combined results from refs 17 and 21 which appear to be most reliable and form the basis of our fit. The lines drawn in Figures 1 and 2 are from the present modeling; see below. While $k_{Rad,0}$ is very well reproduced, our modeling suggests a temperature dependence of $k_{Mol,0}$ which markedly differs from that of eq 18. Likewise, the temperature dependence of the thermal branching ratio is suggested to be weaker than given by the experimental result of

$$k_{Rad,0}/k_0 = 0.69\exp(-2580\ \mathrm{K}/T) \quad (20)$$

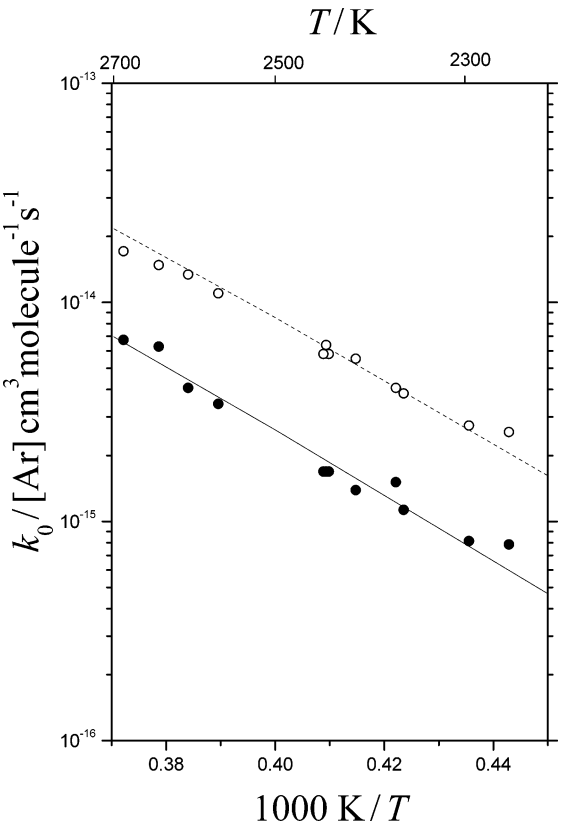

Figure 1. Modeled and experimental rate coefficients $k_{Rad,0}$ and $k_{Mol,0}$. Experiments from ref 21: (●) $k_{Rad,0}$/[Ar] (−) = $k_{Mol,0}$/[Ar]. Modeling from this work: (○) $k_{Rad,0}$/[Ar], (- -) = $k_{Mol,0}$/[Ar] (see text).

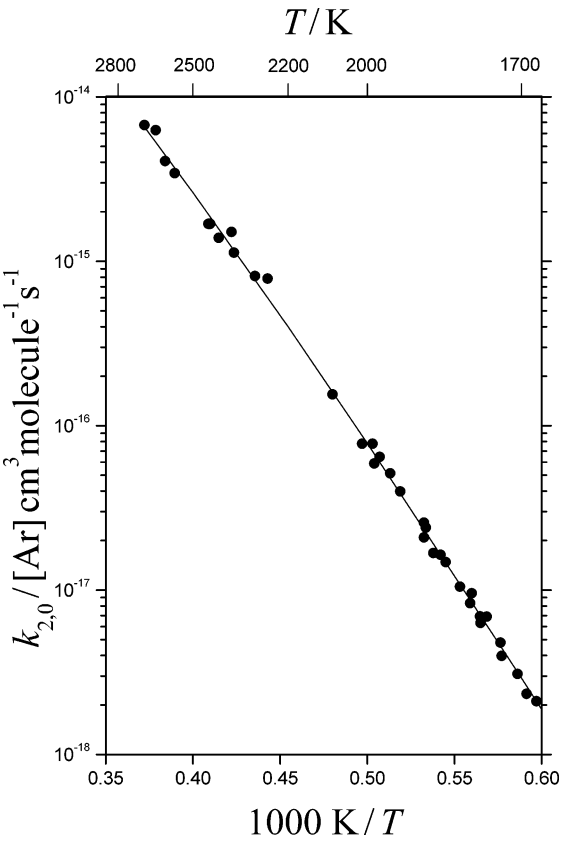

Figure 2. Modeled and experimental rate coefficients $k_{2,0}$ = $k_{Rad,0}$ (modeling from this work, full line; experimental points (●) from refs 17 (T > 2200 K) and from ref 21 (T < 2200 K); see text).

However, the uncertainty of eq 20 is considerable and the measured points also appear consistent with the modeled line, see below.

Absolute value and temperature dependence of k_0 (or of $k_{Rad,0}$), with the modeling results from section III, lead to E_0 = $E_{0,1}(J = 0)$ and $\langle\Delta E\rangle$. At the same time, the Stern−Volmer plots of the quantum yield of formaldehyde photolysis in the spectral range 340−360 nm should be reproduced by the same set of parameters.[20] In this range, the photolysis nearly exclusively is governed by channel 1, either in the tunneling range $E < E_{0,1}$ or at energies $E > E_{0,1}$ but being below the threshold $E_{0,2}$ for channel 2; see below. Pyrolysis and photolysis results in this range, therefore, should be reproduced equally well. It was shown in ref 20 that this is indeed the case.

The modeling with the expressions from section III employs the molecular parameters given in the Appendix of ref 6, except that the present more refined calculation of the rotational factors F_{rot} with eq 8 leads to F_{rot} = 2.39, 2.33, 2.21, 2.13, and 1.95 at T = 1400, 1700, 2000, 2500, and 3200 K instead of F_{rot} = 8.1, 7.2, 6.2, 4.8, and 3.5 from ref 6, respectively. The latter values were obtained with the simple standard approximation for F_{rot} which applies to single-channel reactions; see ref 22. The present procedure with eq 8 more properly accounts for rotational channel switching; because of the markedly changing J dependence of $E_{0,min}(J)$ at $J = J_{sw}$, the Waage−Rabinovitch interpolation scheme for F_{rot} used in ref 22 becomes inadequate. One realizes that considerable differences are obtained, partly because of the use of different ways to calculate F_{rot} partly because of the revised[23] values of C_ν and ν.

Employing the described improved F_{rot} and the new data for $k_{Mol,0}$, the results shown in Figures 1 and 2 are well fitted by the present modeling with $E_{0,1}(J = 0)$ = 81.7 kcal mol^{-1}, $-\langle\Delta E\rangle$/hc = 100 cm^{-1} and C_2 = 0.0030 such as illustrated by the lines in the figures. The uncertainty of $E_{0,1}$ from the temperature dependence in Figure 2 is estimated to be about ±0.5 kcal mol^{-1}, which confirms the value of 81.9(±0.3) kcal mol^{-1} recommended in ref 19. Fixing k_0(2500 K) to the experimental value of k_0 = [Ar] 1.11 × 10^{-14} cm^3 molecule^{-1} s^{-1}, varying E_0 between 79, 81, and 83 kcal/mol^{-1}, would lead to values of $-\langle\Delta E\rangle$/hc = 78, 98, and 120 cm^{-1}, respectively. The uncertainty of $-\langle\Delta E\rangle$/hc is thus estimated to be given by the experimental uncertainty of $k_{Mol,0}$ (2500 K), i.e. ±25%. The value of $\langle\Delta E\rangle$ derived from the absolute value of k_0 is in line with the results from the Stern−Volmer plots of the quantum yields,[20] for which $-\langle\Delta E\rangle$/hc = 80(±40) cm^{-1} was derived in the bath gas N_2 (employing the same anharmonicity factors F_{anh}), and with results for similar reaction systems, e.g., the dissociation of CH_4 in Ar which led[36] to $-\langle\Delta E\rangle$/hc = 50 cm^{-1}. The dependence of the thermal branching ratio $V_{Rad}(T)$ on the parameter C_2, on the other hand, is illustrated in the Appendix. Keeping $E_{0,1}(J = 0)$ and $\langle\Delta E\rangle$ fixed, such as given by the foregoing analysis of k_0, the experimental value of V_{Rad}(2500 K) is best reproduced by C_2 = 0.0030; see Appendix. At the same time the modeled temperature dependence is weaker than the experimental result of eq 20. With the chosen set of parameters (see the second equation in case i of the Appendix), the modeling result over the range 1700−2700 K is represented by

$$V_{Rad}(T) = k_{Rad,0}/k_0 = 0.0111\ T^{0.39} = 0.333\ \exp(-871\ \mathrm{K}/T) \quad (21)$$

The given value of C_2 appears to be smaller than the value C_2 = 0.05 obtained by a fit to the photolysis quantum yields[20] in the range 310−340 nm. Although being still within the experimental uncertainty,[20] this difference of the fitted C_2 values may point toward some differences in the character of the

TABLE 1: Modeled Low-Pressure Rate Coefficients of Formaldehyde Pyrolysis (in cm^3 molecule^{-1} s^{-1})

T/K	$k_{Rad,0}$/[Ar]	$k_{Mol,0}$/[Ar]
1200	1.9×10^{-22}	9.0×10^{-22}
1400	2.2×10^{-20}	9.6×10^{-20}
1700	2.9×10^{-18}	1.2×10^{-17}
2000	7.8×10^{-17}	2.9×10^{-16}
2200	4.0×10^{-16}	1.4×10^{-15}
2500	2.6×10^{-15}	8.5×10^{-15}
2700	7.0×10^{-15}	2.2×10^{-14}
3200	4.2×10^{-14}	1.2×10^{-13}
3500	8.9×10^{-14}	2.4×10^{-13}

excitation processes (collisional vs photoexcitation), see ref 24. However, apart from this small difference the branching ratios from pyrolysis and photolysis appear to be fully consistent.

One final remark concerns the only weak dependence of $V_{Rad}(T)$ on the average energy $\langle\Delta E\rangle$ transferred per collision. If there were no rotational channel switching, one should expect[34] a stronger dependence of $\langle\Delta E\rangle$ such as also characterized by the "collisional competitive reaction spectroscopy" of refs 38 and 39. In the present case, however, a major part of $k_{2,0}$ arises from rotational states with $J > J_{sw}$ where channels 2 and 3 are energetically most favorable and channel 1 is only of minor importance (if it can be separated at all from channel 3). In this case, energy transfer is relevant only through its sampling of the specific branching ratio $V_{Rad}(E,J)$ and not through its overcoming of the energy gap $\Delta E = E_{0,2} - E_{0,1}$. On the other hand, the strong dependence of V_{Rad} on ΔE_0, which was exploited in ref 6, is confirmed by the modeling illustrated in the Appendix.

VI. Representation of Rate Coefficients

The modeling results from section V, employing $E_{0,1}(J = 0) = 81.7$ kcal mol^{-1}, $-\langle\Delta E\rangle/hc = 100$ cm^{-1}, and $C_2 = 0.0030$, are summarized in Table 1 and illustrated by the lines in Figures 1 and 2. They can be approximated over the range 1700−2700 K by the expressions

$$k_{Mol,0}/[Ar] = 4.3 \times 10^3\, T^{-3.1} \exp(-41110\ \mathrm{K}/T)\ \mathrm{cm^3\ molecule^{-1}\ s^{-1}} \quad (22)$$

and

$$k_{Rad,0}/[Ar] = 5.6 \times 10^1\, T^{-2.7} \exp(-41110\ \mathrm{K}/T)\ \mathrm{cm^3\ molecule^{-1}\ s^{-1}} \quad (23)$$

where the exponential factor corresponds to $\exp(-E_0/kT)$. The uncertainty of the absolute values from these rate coefficients is estimated to be ±25% such as estimated in refs 17 and 21. Because of the non-Arrhenius form of the rate constants, the deviation of the representation by eqs 22 and 23 from the detailed modeling increases to more than 50% at the limits of the considered temperature range 1200−3500 K. Outside the range 1700−2700 K, therefore, Table 1 should be used instead of eqs 24 and 23. Alternatively, abandoning the exponential factor $\exp(-E_0/kT)$, the expressions

$$k_{Mol,0} = 7.3 \times 10^{14}\, T^{-6.1} \exp(-47300\ \mathrm{K}/T)\ \mathrm{cm^3\ molecule^{-1}\ s^{-1}} \quad (24)$$

and

$$k_{Rad,0} = 2.1 \times 10^{12}\, T^{5.5} \exp(-47300\ \mathrm{K}/T)\ \mathrm{cm^3\ molecule^{-1}\ s^{-1}} \quad (25)$$

within better than 4% reproduce the modeled data over the full range 1200−3500 K and, therefore, are recommended for practical applications.

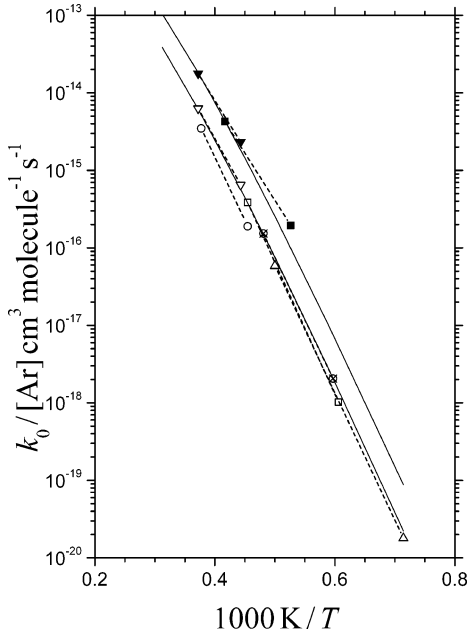

Figure 3. Modeled and experimental rate coefficients $k_{Rad,0}$ (lower curves) and $k_{Mol,0}$ (upper curves) of formaldehyde pyrolysis (full lines, modeling from this work; dashed lines with symbols marking the ends of the studied temperature ranges, experiments from refs 12 (○), 13 (▼ and ▽), 15 (⊗), 17 (△), and 21 (■ and □); modeling fitted to results from refs 17 and 21; see text).

The present fitting of parameters relied on the experiments from refs 17 and 21, but the general agreement with data from other publications is also quite satisfactory. Figure 3 compares the results from refs 17 and 21 and from the present modeling with other experiments in the bath gas Ar. One should note that the shown symbols are not experimental points but labels indicating the ranges of the experimental data. The general agreement for measurements of $k_{Rad,0}$ is quite satisfactory. The data from ref 21 and from the present modeling now also complete the base for $k_{Mol,0}$ which is much more difficult to measure.

In the future, more experiments on the pressure dependence as well as modeling of the branching ratio over the full falloff curve appear desirable. The earlier attempts from ref 17 neglected channel 3 and, therefore, appear obsolete. The modeling to be done will employ specific rate constants $k(E,J)$ for all dissociation pathways, such as elaborated in ref 40, within a suitable solution of the master equation.

VII. Conclusions

The present analysis of the low-pressure rate coefficients of the thermal dissociation of formaldehyde into radical and molecular products provides results which are internally consistent with representations of the quantum yields for formaldehyde photolysis over the wavelength range 310−360 nm. The modeling is consistent with the "high" value $E_{0,1}(J = 0) = 82.2$-(±0.3) kcal mol^{-1} for the threshold energy of the molecular elimination channel 1. The fitted value of $-\langle\Delta E\rangle/hc = 100(\pm 20)$ cm^{-1} for the bath gas Ar appears to be of normal magnitude and is consistent with a value of $-\langle\Delta E\rangle/hc = 80(\pm 40)$ cm^{-1} for the bath gas N_2 such as derived from photolysis quenching experiments. One should notice, however, that it relies on the absolute values of the experimental rate

coefficients at 2500 K, here taken from ref 21. In addition, it relies on the details of the rotational factors F_{rot} such as calculated in the present work and on the anharmonicity factors F_{anh} such as modeled in ref 6. There appears to be a minor difference in the J dependence of the fitted energy and angular momentum specific branching ratios derived from the pyrolysis and photolysis experiments. This is still within the experimental uncertainty but it may also be due to a slight difference in the respective excitation pathways such as discussed in refs 20 and 24. Equations 22 and 23 appear to be the presently most appropriate expressions for characterizing formaldehyde pyrolysis in combustion chemistry.

Acknowledgment. The author thanks James A. Miller for many stimulating discussions of combustion reactions. He also thanks S. D. Chambreau and J. M. Bowman for a preprint of ref 5 as well as V. Vasudevan and R. K. Hanson for a preprint of ref 21. Financial support of this work by the Deutsche Forschungsgemeinschaft (SFB 357 "Molekulare Mechanismen unimolekularer Prozesse") is also gratefully acknowledged.

Appendix

Modeled Thermal Branching Ratios $V_{Rad,0} = k_{2,0}/k_0$. Modeling with fixed parameters $E_{0,1}(J = 0) = 81.7$ kcal mol^{-1}, $E_{0,2}(J = 0) = 86.71$ kcal mol^{-1}, $-\langle\Delta E\rangle/hc = 100$ cm^{-1}, $C_1 = 0.75$, and $C_3/hc = 750$ cm^{-1}.

$$C_2 = 0.0: \quad V_{Rad} = 0.149, 0.163, 0.185, 0.193$$

$$C_2 = 0.003: \quad V_{Rad} = 0.213, 0.225, 0.244, 0.252$$

$$C_2 = 0.006: \quad V_{Rad} = 0.264, 0.275, 0.292, 0.299$$

$$C_2 = 0.05: \quad V_{Rad} = 0.469, 0.476, 0.487, 0.491$$

The values of V_{Rad} are modeled for $T = 1700$, 2000, 2500, and 2700 K respectively, see text; The second equation in case 1 denotes the finally chosen set of parameters.

References and Notes

(1) Van Zee, R. D.; Foltz, M. F.; Moore, C. B. *J. Chem. Phys.* **1993**, *99*, 1664.
(2) Townsend, D.; Lahankar, S. A.; Lee, S. K.; Chambreau, S. D.; Suits, A. G.; Zhang, X.; Rheinecker, J.; Harding, L. B.; Bowman, J. M. *Science* **2004**, *306*, 1158.
(3) Zhang, X.; Rheinecker, J. L.; Bowman, J. M. *J. Chem. Phys.* **2005**, *122*, 11431.
(4) Bowman, J. M.; Zhang, X. *Phys. Chem. Chem. Phys.* **2006**, *8*, 321.
(5) Lahankar, S. A.; Chambreau, S. D.; Zhang, X.; Bowman, J. M.; Suits, A. G. *J. Chem. Phys.* **2006**, submitted for publication.
(6) Troe, J. *J. Phys. Chem. A* **2005**, *109*, 8320. (The values for C_ν and ν in ref 6 were calculated by an oversimplified method which turned out to be inadequate; these values as well as Figure 2 therefore should be rejected. The present values for C_ν and ν are from trajectory calculations of ref 40 performed on the ab initio potential of ref 28.)
(7) Moortgat, G. K.; Warneck, P. *J. Chem. Phys.* **1979**, *70*, 3639.
(8) Moortgat, G. K.; Seiler, W.; Warneck, P. *J. Chem. Phys.* **1983**, *78*, 1185.
(9) Smith, G. D.; Molina, L. T.; Molina, M. J. *J. Chem. Phys. A* **2002**, *106*, 1233.
(10) Sander, S. P.; Friedl, R. R.; Golden, D. M.; Kurylo, M. J.; Huie, R. E.; Moortgat, G. K.; Keller-Rudek, H.; Wine, P. H.; Ravishankara, A. R.; Kolb, C. E.; Molina, M. J.; Finlayson-Pitts, B. J.; Orkin, V. L. *NASA-JPL Evaluation No. 15, 2006, JPL Publication 06−2*; JPL: Pasadena, CA, 2006.
(11) Atkinson, R.; Baulch, D. L.; Cox, R. A.; Crowley, J. N.; Hampson, R. F.; Hynes, R. G.; Jenkin, M. E.; Rossi, M. J.; Troe, J. *Atmos. Chem. Phys.* **2006**, *0*, 000.
(12) Saito, K.; Kakumoto, T.; Nakanishi, Y.; Imamura, A. *J. Phys. Chem.* **1985**, *89*, 3109.
(13) Rimpel, G.; Just, T. Unpublished data cited In Baulch, D. L.; Cobos, C. J.; Cox, R. A.; Esser, C.; Frank, P.; Just, T.; Kerr, J. A.; Pilling, M. J.; Troe, J.; Walker, R. W.; Warnatz, J. *J. Phys. Chem. Ref. Data* **1992**, *21*, 411.
(14) Irdam, E. A.; Kiefer, J. H.; Harding, L. B.; Wagner, A. F. *Int. J. Chem. Kinet.* **1993**, *25*, 285.
(15) Hidaka, Y.; Taniguchi, T.; Tanaka, H.; Kamesawa, T.; Inami, K.; Kawano, H. *Combust. Flame* **1993**, *92*, 365.
(16) Kumaran, S. S.; Carroll, J. J.; Michael, J. V. *Proc. Combust. Inst.* **1998**, *27*, 125.
(17) Friedrichs, G.; Davidson, D. F.; Hanson, R. K. *Int. J. Chem. Kinet.* **2004**, *36*, 157.
(18) Polik, W. F.; Guyer, D. R.; Moore, C. B. *J. Chem. Phys.* **1990**, *92*, 3453.
(19) Feller, D.; Dupuis, M.; Garrett, B. C. *J. Chem. Phys.* **2000**, *113*, 218.
(20) Troe, J. *J. Phys. Chem. A*, **2007**, *111*, 3868.
(21) Vasudevan, V.; Davidson, D. F.; Hanson, R. K.; Bowman, C. T.; Golden, D. M. *Proc. Combust. Inst.* **2007**, *31*, submitted for publication.
(22) Troe, J. *J. Phys. Chem.* **1979**, *83*, 114.
(23) Farnum, J. D.; Zhang, X.; Bowman, J. M. *J. Chem. Phys.* **2007**, submitted for publication.
(24) Pope, F. D.; Smith, C. A.; Davis, P. R.; Shallcross, D. E.; Ashfold, M. N. R.; Orr-Ewing, A. J. *Faraday Discuss., Chem. Soc.* **2005**, *130*, 59.
(25) Goddard, J. D.; Schaefer, H. F. *J. Chem. Phys.* **1979**, *70*, 5117.
(26) Gray, S. K.; Miller, W. H.; Yamaguchi, Y.; Schaefer, H. F. *J. Am. Chem. Soc.* **1981**, *103*, 1900.
(27) Yamaguchi, Y.; Wesolowski, S. S.; Van, Huis, T. J.; Schaefer, H. F. *J. Chem. Phys.* **1998**, *108*, 5281.
(28) Zhang, X.; Zou, S.; Harding, L. B.; Bowman, J. M. *J. Phys. Chem. A* **2004**, *108*, 8980.
(29) Yonehara, T.; Kato, S. *J. Chem. Phys.* **2002**, *117*, 11131.
(30) Terentis, A. C.; Kable, S. H. *Chem. Phys. Lett.* **1996**, *258*, 626.
(31) Terentis, A. C.; Waugh, S. E.; Metha, G. F.; Kable, S. H. *J. Chem. Phys.* **1998**, *108*, 3187.
(32) Forst, W. *J. Phys. Chem.* **1983**, *87*, 4489, 5234.
(33) Schecker, H. G.; Jost, W. *Ber. Bunsen-Ges. Phys. Chem.* **1969**, *73*, 521.
(34) Just, T.; Troe, J. *J. Phys. Chem.* **1980**, *84*, 3068.
(35) Troe, J. *J. Chem. Phys.* **1977**, *66*, 4758.
(36) Cobos, C. J.; Troe, J. *Z. Phys. Chem.* **1992**, *176*, 161.
(37) Yonehara, T.; Kato, S. *J. Chem. Phys.* **2006**, *125*, 084307.
(38) Klein, I. E.; Rabinovitch, B. S.; Jung, K. H. *J. Chem. Phys.* **1977**, *67*, 3833.
(39) Klein, I. E.; Rabinovitch, B. S. *J. Phys. Chem.* **1978**, *82*, 243.
(40) Bowman, J. M.; Harding, L. B.; Troe, J.; Ushakov, V. G. Work in progress.